Experimental studies of N/Z equilibration in peripheral collisions using fragment yield ratios

A. L. Keksis,[1,2,*] L. W. May,[1,2] G. A. Souliotis,[1,3,†] M. Veselsky,[1,4] S. Galanopoulos,[1,‡] Z. Kohley,[1,2] D. V. Shetty,[1,§] S. N. Soisson,[1,2] B. C. Stein,[1,2] R. Tripathi,[1] S. Wuenschel,[1,2] S. J. Yennello,[1,2] and B. A. Li[5]

[1]*Cyclotron Institute, Texas A&M University, College Station, Texas 77843, USA*

[2]*Chemistry Department, Texas A&M University, College Station, Texas 77843, USA*

[3]*Laboratory of Physical Chemistry, Department of Chemistry, National and Kapodistrian University of Athens, Panepistimiopolis, Athens GR-15771, Greece*

[4]*Institute of Physics, Slovak Academy of Sciences, Bratislava, Slovakia*

[5]*Department of Physics, Texas A&M University-Commerce, Commerce, Texas 75429, USA*

(Received 11 February 2010; published 17 May 2010)

Peripheral collisions of ^{40}Ca and ^{48}Ca projectiles at 32 MeV/nucleon on ^{112}Sn and ^{124}Sn targets were studied in this work. The fragments of the projectile-like source (quasiprojectile) were collected with a charged-particle multidetector array. The average value of the neutron-to-proton ratio N/Z of the quasiprojectiles formed in the reactions was determined with two approaches. The first is a direct reconstruction approach using isotopically resolved fragments and is hindered by undetected neutrons leading to lower N/Z values. The second approach, based on the assumption of early fragment formation, employs yield ratios of fragment isobars and is not hindered by undetected neutrons. Using this approach, the amount of N/Z mixing that occurred in the quasiprojectiles (compared to a fully N/Z equilibrated system) was found to be approximately 53%. The experimental results were compared with model calculations. First, the phenomenological DIT (deep inelastic transfer) model was used, followed by the statistical multifragmentation model (SMM). The results of these calculations are in close agreement with the data and indicate that the mean number of undetected neutrons increases with the N/Z of the composite system, accounting for the difference observed between the two approaches of quasiprojectile N/Z determination. Second, the microscopic transport model IBUU (isospin-dependent Boltzmann-Uehling-Uhlenbeck) was employed, providing preliminary results in reasonable agreement with the data. The determination of the degree of N/Z equilibration employing the present fragment yield ratio approach may provide a valuable probe to study the isospin part of the nuclear equation of state in conjunction with detailed microscopic models of the collisions in the Fermi energy regime.

DOI: 10.1103/PhysRevC.81.054602 PACS number(s): 25.70.Mn, 25.70.Pq

I. INTRODUCTION

Detailed studies of the isospin degree of freedom in nuclear reactions provide valuable probes of the different formulations of the nuclear equation of state and especially its isospin-dependent part [1–10]. More specifically, the study of the process of N/Z equilibration has attracted much attention because of the intimate connection with the isospin part of the equation of state [8]. Various authors have used a number of experimental approaches to study N/Z equilibration in central heavy-ion collisions including multisource fitting of fragment energy spectra [11], rapidity [12], baryon energy deficit [13], transverse energy distributions [14], quadrupole moments [14], isotope tracer method [15], and isobaric yield ratios in symmetric systems [16]. Early work on N/Z equilibration revealed two main processes involved, drift and diffusion [17,18]. Drift is caused by the density gradients of the neutrons and protons in the participant zone (i.e., interaction region), while diffusion is caused by the difference in N/Z of the target and the projectile [19]. Recently, the isoscaling approach in heavy-residue data has been shown to provide a sensitive probe of the process of N/Z equilibration as a function of energy dissipation [20,21]. Along these lines, peripheral reactions in the Fermi energy regime have been found to produce very neutron-rich sources and, apart from the opportunity of accessing exotic nuclei, they offer a useful route to study the degree of N/Z transport and equilibration [22–27].

In this work peripheral collisions of asymmetric systems in the Fermi energy regime were studied to determine the degree of N/Z equilibration that took place during the reaction. The reactions studied cover a range of impact parameters from peripheral to midperipheral collisions between the projectile and the target. During the projectile-target interaction, nucleons are exchanged, forming a projectile-like source, termed the quasiprojectile (QP), and a target-like source, termed the quasitarget (QT). A drive toward N/Z equilibrium will end up with both the N/Z of the quasiprojectile and the N/Z of the quasitarget moving toward the N/Z of the composite system, given by the expression

$$\frac{N_{\rm CS}}{Z_{\rm CS}} = \frac{N_P + N_T}{Z_P + Z_T}, \tag{1}$$

*Present address: C-NR, Los Alamos National Laboratory, Los Alamos, New Mexico, 87545, USA.

†Corresponding author: soulioti@comp.tamu.edu, soulioti@chem.uoa.gr

‡Present address: Greek Army Academy, Department of Physical Sciences, Athens, Greece.

§Present address: Physics Department, Western Michigan University, Kalamazoo, MI 49008, USA.

where N_{CS}, N_P, and N_T are the neutron numbers of the composite system, the projectile, and the target, respectively, and Z_{CP}, Z_P, and Z_T are the corresponding proton numbers. The composite system is the system that would form if the projectile and the target were completely combined, and therefore its N/Z represents the N/Z of a fully N/Z (or "chemically") equilibrated system [18,28]. It is obvious that the changes in the N/Z of both the quasiprojectile and the quasitarget sources depend on the degree of N/Z equilibration that occurs during the interaction.

In this work, the mean N/Z of the quasiprojectile source for each reaction system is determined using two different approaches. The first approach uses isotopically resolved charged fragments to reconstruct the quasiprojectile on an event-by-event basis [22,23]. The second approach, developed in this work, uses fragment yield ratios of pairs of isobars to determine the average N/Z of the quasiprojectile [29]. Then, knowing the N/Z of the quasiprojectile, the degree of N/Z equilibration that occurs can be determined according to the expression

$$f_{EQ} = \frac{\left(\frac{N}{Z}\right)_{QP} - \left(\frac{N}{Z}\right)_P}{\left(\frac{N}{Z}\right)_{CS} - \left(\frac{N}{Z}\right)_P}. \quad (2)$$

In this equation, the difference between the quasiprojectile (QP) and projectile (P) N/Z is scaled by the maximum N/Z difference, that is, that between the composite system (CS) N/Z and the projectile (P) N/Z. This equation provides the fraction f_{EQ} of N/Z equilibration (or mixing) that occurs during the projectile-target interaction relative to that of a completely N/Z equilibrated system. It is obvious that if no N/Z equilibration occurs, then the N/Z of the quasiprojectile equals the N/Z of the projectile and Eq. (2) gives $f_{EQ} = 0$. If full N/Z equilibration is reached, then the quasiprojectile N/Z equals the composite system N/Z and, of course, $f_{EQ} = 1$.

This article is organized as follows. In Sec. II, a brief description of the experimental device, the data analysis, and the calibrations is given. In Sec. III, the determination of the quasiprojectile N/Z using the two different approaches is presented. In Sec. IV, theoretical calculations and comparison between the theoretical and experimental results are discussed. Finally, the summary and conclusions are given in Sec. V.

II. EXPERIMENTAL

Beams of ^{40}Ca and ^{48}Ca were accelerated to 32 MeV/nucleon using the K500 superconducting cyclotron at the Cyclotron Institute of Texas A&M University. The targets were enriched ^{112}Sn (1.30 mg/cm^2) and ^{124}Sn (1.15 mg/cm^2). The reaction systems span a wide range in the difference between projectile and target N/Z. Table I lists the reaction systems, the projectile and the target N/Z, and the absolute difference $\Delta(N/Z)$ between the projectile and the target N/Z. The absolute difference is used because in the ^{48}Ca + ^{112}Sn system the projectile N/Z is larger than the target N/Z. Thus, in this case the diffusion is expected to proceed in the opposite direction compared to the rest of the systems studied.

TABLE I. List of systems, projectile N/Z, target N/Z and the absolute difference between target and projectile N/Z.

System	$N/Z_{Projectile}$	N/Z_{Target}	$\Delta(N/Z)$
^{48}Ca + ^{124}Sn	1.40	1.48	0.0800
^{48}Ca + ^{112}Sn	1.40	1.24	0.1600
^{40}Ca + ^{112}Sn	1.00	1.24	0.2400
^{40}Ca + ^{124}Sn	1.00	1.48	0.4800

The fragments were collected with the FAUST multidetector array [22,23,29,30]. FAUST is comprised of 68 detector telescopes arranged in five rings, a cross section of which is shown in Fig. 1. Each detector telescope has a 300-μm Si detector followed by a 3-cm CsI(Tl) crystal. Isotopic resolution was achieved up to oxygen ($Z = 8$), as shown in the ΔE-E spectrum in Fig. 2. This figure is the composite of the data from all systems for a single detector and demonstrates the stability of the detector during the experiment. FAUST has 90% angular coverage from 2.3° to 33.6°, which is ideal for collecting fragments from the breakup of quasiprojectiles coming from heavy-ion reactions in the Fermi energy regime. The high threshold of the detectors effectively blocks fragments originating from the quasitarget, due to their lower momentum [22,29].

The Si detectors were calibrated using a ^{228}Th α source. The energy deposited in the CsI detectors was calibrated using the Birks equation [31]:

$$E = \sqrt{L^2 + 2\rho L[1 + \log(1 + L/\rho)]}. \quad (3)$$

In this equation, the light output (L) and the parameter ρ are used to determine the energy (E) deposited in the CsI detector. The light output has two variables, a pedestal and a scaling parameter, while the ρ parameter is dependent on the mass and charge of the nuclide ($\propto AZ^2$). The parameters are adjusted to attain the best fit using the three nuclides ^{4}He, ^{7}Li, and ^{9}Be. [These three nuclides were selected because they were readily identifiable for the majority of the detector telescopes.] A line was drawn tracing the ΔE-E energy loss for each of the three nuclides and, using a minimization procedure, was fit to energy loss calculations obtained with the code DONNA [32]. Finally, particle identification was accomplished by drawing gates around each nuclide in the ΔE-E spectrum for every detector telescope. Further information on the experimental setup, the calibrations, the gating, and the analysis procedure can be found in Ref. [29].

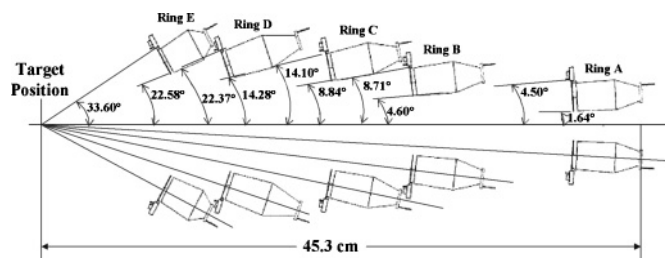

FIG. 1. The cross section of FAUST showing the five rings that hold the 68 ΔE–E detector telescopes.

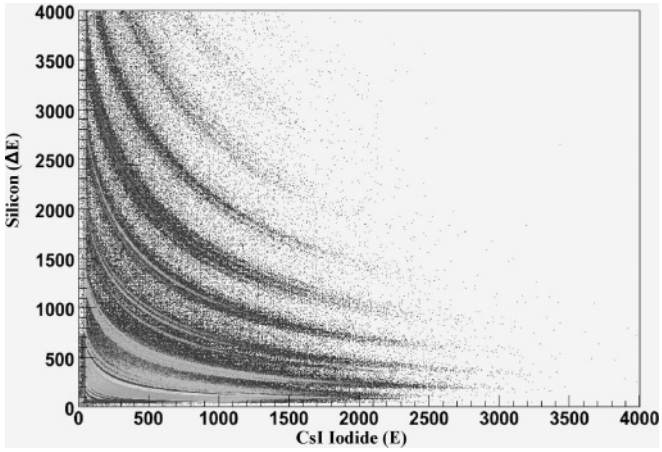

FIG. 2. Example of a silicon versus cesium iodide (ΔE-E) spectrum from a FAUST detector showing isotopic resolution up to oxygen. (Note: Scale on the axes are given in channel numbers).

III. QUASIPROJECTILE N/Z DETERMINATION

A. Quasiprojectile reconstruction approach

The first approach for determining the mean N/Z of the quasiprojectile used the isotopically identified fragments from each event to reconstruct the atomic number $Z_{\rm QP}$ and the mass number $A_{\rm QP}$ of the quasiprojectile [22,29] by summing the atomic numbers Z_f and the mass numbers A_f of all the fragments of the event:

$$Z_{\rm QP} = \sum Z_f, \tag{4}$$

$$A_{\rm QP} = \sum A_f. \tag{5}$$

Since FAUST is a charged-particle detector array, neutrons cannot be detected. As a result, the reconstructed events may have the correct atomic number $Z_{\rm QP}$, but smaller than the actual mass number $A_{\rm QP}$ because of the inability to detect neutrons. The effect of undetected neutrons is determined by employing a two-stage model, discussed further in Sec. IV. The mean quasiprojectile N/Z for each system is then calculated from all reconstructed events and the results are summarized in Table II under the column "N/Z exp. recon." (experimental reconstruction). The reconstruction approach requires as complete as possible angular coverage so that all the fragments from the fragmenting quasiprojectile be collected. Also, because neutrons are not detected and, thus, should be missing from the reconstructed source mass, the calculated quasiprojectile N/Z is lower than the actual N/Z.

B. Isobaric fragment yield ratio approach

The new approach of determining the N/Z of the quasiprojectile employs fragment yield ratios and a fitting procedure that is described in the following [29]. The idea behind the approach is that the fragments are formed with a memory of the N/Z of the quasiprojectile. It is assumed that the time scale for fragment formation is short compared to the fragmentation time scale, so that the neutrons are present when the fragments are formed [33,34]. Thus, the yields of fragments of given N/Z convey information of the N/Z of the source that produces them. As a consequence, the N/Z of the quasiprojectile determined by this approach is essentially not affected by the neutron nondetection (as will be shown later with the help of detailed simulations). Furthermore, we note that the approach does not require full angular coverage. However, it was found that the reconstruction procedure is important to make a clear selection of quasiprojectile sources whose average N/Z is to be determined [29].

The detector arrangement of FAUST provided fragment data at 13 distinct angles. In the present article only the data at the angle of 7° is shown because they correspond to the highest statistics. The data obtained at the other angles show similar trends and can be found in Ref. [29]. As an example of isotope distributions, the fractional yields of carbon isotopes from all systems are shown in Fig. 3. For completeness, we note that to obtain the fractional yield of an isotope of a given element, the yield of the isotope is scaled by the sum of the yields of all produced isotopes of that element. In Fig. 3, we observe that the most neutron-rich systems preferentially populate the most neutron-rich isotopes and, correspondingly, the most proton-rich systems populate the most proton-rich isotopes. This trend, present in all the fractional yields from hydrogen to oxygen of the present work [29], is consistent with other data in the literature (e.g., Ref. [35]).

To proceed with the implementation of the new approach, yield ratios for the isobar pairs with $A = 3$, 6, 7, 11, 14, and 16 were obtained from the four reactions. (The above isobars were chosen as they showed yield ratios consistent between the various detectors of the array [29].) As a first step, these isobar yield ratios are plotted individually versus the N/Z of the composite system for the four systems in the upper panel of Fig. 4. This figure shows that the isobaric yield ratios are not linearly dependent on the N/Z of the composite

TABLE II. Summary of results from DIT/SMM and IBUU comparisons with the experimental data (see text).

System	N/Z target	N/Z projectile	N/Z comp. sys.	N/Z exp. recon.	N/Z exp. fit.	N/Z sim. recon.	N/Z sim. fit.	N/Z DIT prim.	Neutron loss	N/Z IBUU prim.
^{40}Ca + ^{112}Sn	1.24	1.00	1.17	0.98	1.09	0.97	1.11	1.04	2.31	1.12
^{40}Ca + ^{124}Sn	1.48	1.00	1.34	0.99	1.18	1.00	1.22	1.12	2.86	1.22
^{48}Ca + ^{112}Sn	1.24	1.40	1.29	1.03	1.34	1.08	1.33	1.27	5.19	1.25
^{48}Ca + ^{124}Sn	1.48	1.40	1.46	1.05	1.43	1.13	1.44	1.39	6.10	1.34

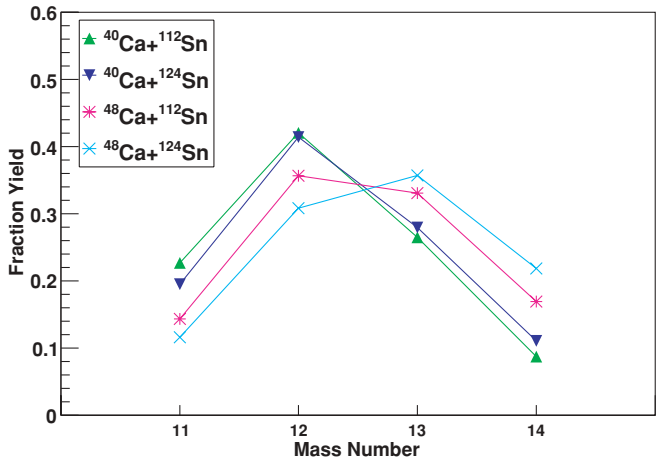

FIG. 3. (Color online) Carbon fractional yields from the four reaction systems at 32 MeV/nucleon. The neutron-rich systems preferentially populate the most neutron-rich isotopes.

system. However, they are arranged in two distinct regions: one corresponding to the reactions with the ^{112}Sn target and the other to those with the ^{124}Sn target.

Furthermore, it was assumed that the N/Z of the quasiprojectile $(N/Z)_{\rm QP}$ can be expressed as a linear combination (mixing) between the N/Z of the projectile and the N/Z of the target, that is,

$$(N/Z)_{\rm QP} = k_P\,(N/Z)_P + k_T(N/Z)_T. \qquad (6)$$

The two variables k_P and k_T represent the corresponding fractions of N/Z coming from the projectile and the target, respectively, and thus should obey the constraint $k_P + k_T = 1$. The variables k_P and k_T were determined by an optimization procedure in which the best linear dependence of each isobaric yield ratio with respect to $(N/Z)_{\rm QP}$ [given by Eq. (6)] was determined simultaneously for the four systems. The optimization procedure was implemented in two ways: first, individually for each isobar ratio and, second, globally, for all six isobars simultaneously. Using the values of k_P and k_T, the value of $(N/Z)_{\rm QP}$ was obtained for the resulting quasiprojectile from each of the four systems. The results of the global optimization procedure are given in Table II under the column "N/Z exp. fit." (experimental fitting). In the lower part of Fig. 4, the isobar yield ratios are plotted versus the optimum N/Z of the quasiprojectile $(N/Z)_{\rm QP}$ from the global optimization. For each isobar pair, a (nearly) linear dependence of the yield ratio with respect to $(N/Z)_{\rm QP}$ is observed as a result of the above-mentioned optimization procedure based on Eq. (6).

From Table II we observe that the $(N/Z)_{\rm QP}$ values determined by the fragment yield ratio approach are larger than the values obtained from the reconstruction approach, but they are not close to the corresponding values at full N/Z equilibrium (i.e., composite system N/Z).

In Fig. 5, the degree of equilibration $f_{\rm EQ}$, calculated from the values of $(N/Z)_{\rm QP}$ obtained with the optimization procedure applied individually for each isobar, are plotted as a function of the isobar mass. We notice that there are fluctuations from isobar to isobar, but within experimental uncertainties, we may say that $f_{\rm EQ}$ does not depend on isobar

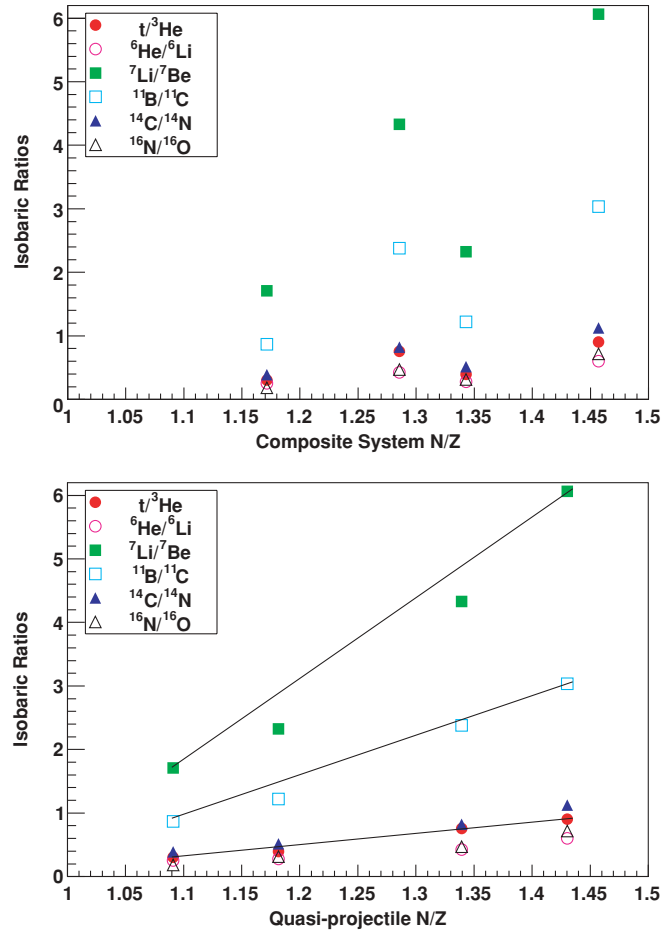

FIG. 4. (Color online) Isobaric yield ratios plotted as a function of the composite system N/Z (upper panel) and quasiprojectile system N/Z after the global optimization procedure [based on Eq. (6)] was applied as described in the text (lower panel). The lines are to guide the eye.

mass. The horizontal line in the figure indicates the value $f_{\rm EQ} = 0.53$ that results from the global optimization procedure and is lower than the individual points. At present we do not have a satisfactory explanation for the difference between the individual points (with an average of $f_{\rm EQ} = 0.65$) and the global line at $f_{\rm EQ} = 0.53$. However, in the following we focus on the results from the global optimization, which, we think, may better reflect the average extent of equilibration for the systems studied.

Finally, in Fig. 6 we give one more representation of the extent of equilibration by the value of $(N/Z)_{\rm QP}$ (from the global optimization, as stated above) scaled by $(N/Z)_{\rm CS}$ as a function of the absolute difference between the target and the projectile N/Z. The N/Z of the quasiprojectile is, as expected, between the N/Z of the projectile and that of the composite system. This representation gives a measure of the average extent of equilibration for each system and is rather insensitive to possible variations between isotope pairs (as also discussed above in relation to Fig. 5).

At this point we wish to remark that according to experimental data on isobaric yield ratios with respect to

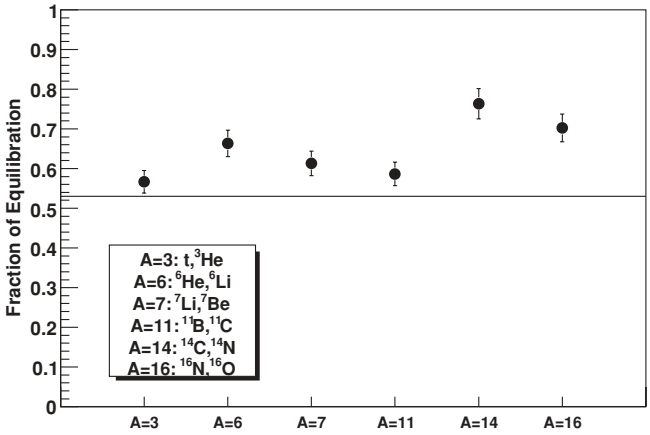

FIG. 5. Dependence of the degree of equilibration f_{EQ} (determined individually for each isobar pair) on the mass of the isobar pair used in the yield ratio approach. The horizontal line ($f_{EQ} = 0.53$) is from the global optimization procedure (see text).

reconstructed source N/Z [36], as well as macrocanonical and canonical descriptions of fragment formation [37,38], we expect that the isobaric yield ratios depend exponentially on the N/Z of the quasiprojectile source. Thus, a linear relationship of the logarithm of the yield ratio with respect to $(N/Z)_{QP}$ is well justified. We tested the aforementioned optimization procedure employing the logarithm of the yield ratios and we observed no essential difference in the results of the $(N/Z)_{QP}$ determination. Thus, the linear dependence of the isobaric yields with respect to $(N/Z)_{QP}$ assumed in the present work seems to be a good approximation of the exponential relation for the range of $(N/Z)_{QP} = 1.1$–1.5 relevant to the present work. However, we stress that application of the present approach to a larger range of $(N/Z)_{QP}$ (as expected from reactions with radioactive beams) may necessitate the use of the exponential relation in the optimization procedure. Finally, before presenting comparisons of the experimental results to model calculations, we note that, apart from the isobaric yield ratios employed in this article, the present yield ratio approach can be implemented using other appropriately chosen yield ratios (e.g., isotopic yield ratios) as described in Ref. [29].

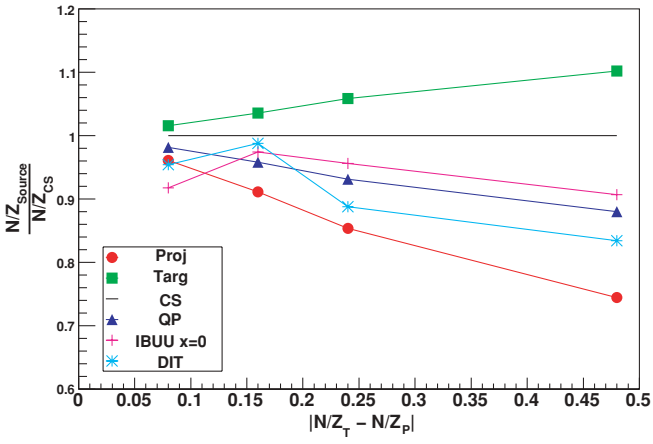

FIG. 6. (Color online) Scaled N/Z of quasiprojectile (from the global optimization procedure), projectile, and target to the N/Z of the composite system as a function of the difference in N/Z between the projectile and the target (see text).

IV. COMPARISONS TO THEORETICAL MODELS

In this section, the experimental results obtained in the present work are compared to theoretical simulations using two kinds of models. First, the phenomenological DIT (deep inelastic transfer model) followed by the statistical multifragmentation model (SMM) and, second, the microscopic transport model IBUU (isospin-dependent Boltzmann-Uehling-Uhlenbeck). A brief description of each model is given followed by the comparison of the theoretical results with the data.

A. DIT/SMM calculations

The phenomenological calculations are based on a two-stage Monte Carlo approach. The dynamical stage of the collision was described by the DIT (deep-inelastic transfer) code of Tassan-Got and Stephan [39] simulating stochastic nucleon exchange in peripheral and semiperipheral collisions. This model has been successful in describing the N/Z, excitation energy, and kinematical properties of excited quasiprojectiles in a number of studies at Fermi energies [20,24,40,41]. The average N/Z of the quasiprojectiles generated by the DIT code is listed under the column "N/Z DIT prim." (DIT primary fragment) in Table II and it is in reasonable agreement with the experimental values from the yield ratio fitting approach (see discussion later).

The quasiprojectiles were then deexcited using a recent version of the statistical multifragmentation model (SMM) [42–47] that is briefly summarized below. The SMM assumes statistical equilibrium at a low-density freeze-out stage. It includes all breakup channels ranging from the compound nucleus to vaporization (channels with only light particles $A < 4$), allowing a unified description of nuclear disintegration with increasing excitation. In the microcanonical treatment, the statistical weight of a decay channel is calculated as an exponential of the entropy of the system in this channel. The model generates a Markov chain of partitions (by employing the Metropolis algorithm) representative of the whole partition ensemble. The Coulomb interaction energy is directly calculated for each spatial configuration of fragments in the freeze-out volume. Standard parameters of the SMM code are employed in the calculations (see also Ref. [29]). In particular, a multiplicity-dependent parametrization of the free volume (determining the contribution of the fragment translational motion to the partition probability [42]) is used, whereas the freeze-out volume (defining the Coulomb energy of the fragment partition) is taken to be six times the nuclear volume at normal density. Finally, the symmetry energy coefficient of the hot fragments assumes its standard liquid-drop value of $C_{sym} = 25$ MeV [29].

The final fragments produced by the SMM code were then passed through a software replica of the FAUST array, which takes into account the angular acceptance of the array and

the energy thresholds of the detectors. In addition, it discards neutrons, because, as mentioned earlier, neutrons were not detected experimentally. The results obtained from the aforementioned filtering procedure were then analyzed using exactly the same procedures that were followed to analyze the experimental data, as described previously. Specifically, to obtain the N/Z of the quasiprojectiles, both the quasiprojectile reconstruction approach and the isobaric yield ratio fitting approach were employed. The results are given in Table II with the QP reconstruction results under column "N/Z sim. recon." (simulation reconstruction) and the yield ratio fitting results under column "N/Z sim. fit" (simulation fitting).

As we see, the results from the simulated QP reconstruction approach are in reasonable agreement with the experimental reconstruction results and they clearly reflect the effect of the neutron nondetection in the determination of the N/Z of the quasiprojectile using the QP reconstruction procedure.

Similarly, the results of the simulated yield ratio fitting approach are in agreement with the corresponding experimental results using this method. By comparing the DIT N/Z results with those from the yield ratio fitting approach, we observe that DIT gives results that are about 5% lower than the values obtained by the yield ratio fitting method applied to the DIT primary results. This difference may be due, in part, to a contribution of the filtering procedure and the detector thresholds applied to the DIT/SMM results. Also, a role may be played by the inadequate description of the nuclear periphery (neutron skin) of the target nuclei in DIT, as pointed out in recent works [24,48].

Table II also shows the extent of the neutron loss as obtained from the simulation (column "neutron loss"), which provides clear evidence for the discrepancy in the N/Z between the QP reconstruction and the yield ratio fitting approaches. Table II shows the expected trend that more neutrons are lost from the more neutron-rich systems. This is also shown in Fig. 7, which presents the correlation of the N/Z of the quasiprojectile from DIT (vertical axis) versus the N/Z of the quasiprojectile reconstructed from SMM after filtering of the fragments through the FAUST filter for the ^{40}Ca + ^{112}Sn system (upper panel) and the ^{48}Ca + ^{124}Sn system (lower panel). Similar behavior has been observed for the other two systems of this work [29].

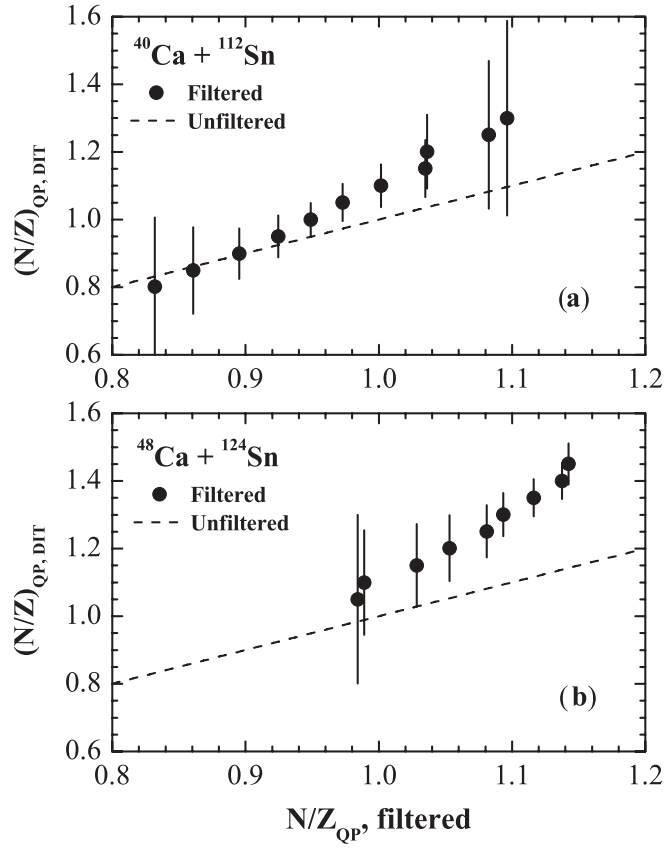

FIG. 7. Correlation of the N/Z of the DIT quasiprojectiles (vertical axis) with the N/Z of the DIT/SMM/filtered (reconstructed) quasiprojectiles for the 32 MeV/nucleon ^{40}Ca + ^{112}Sn (upper panel) and ^{48}Ca + ^{124}Sn (lower panel) systems. The dotted line represents the N/Z of the quasiprojectile if no neutrons were lost (see text).

B. IBUU calculations

To use our experimental results on quasiprojectile N/Z and the degree of N/Z equilibration to probe the isospin part of the nuclear equation of state, comparisons with appropriate microscopic models will be necessary. Such models employ various parametrizations of the effective nucleon-nucleon interaction and provide descriptions of the full dynamical process of the projectile-target interaction [1,49,50].

As a first step toward this goal we performed preliminary calculations with a recent version of the IBUU transport code [10] in which the isospin and momentum-dependent mean-field potential Momentum Dependent Interaction (MDI) is employed [1,9,10]. The code is implemented with the test particle method. The code gives test particle positions, momenta, and identity (proton or neutron, originally target or projectile) at each time step of the calculation. For peripheral and midperipheral collisions, the calculation was stopped at 100 fm/c and the test particle information was used to locate the high-density center of the resulting quasiprojectile. Subsequently, a spherical geometry cut was applied to define and select the quasiprojectile whose N/Z value was determined. The IBUU calculations were performed at impact parameters of $b = 5$, 6, 7, 8, 9, and 10 fm with the $x = 0$ parametrization of the MDI mean-field (corresponding to a stiff density dependence of the nuclear symmetry energy). Because the experimental impact parameter distribution is not known, the $(N/Z)_{QP}$ values for the six impact parameters from IBUU were appropriately averaged (using a triangular distribution with respect to impact parameter) and used for comparison to the data.

First, the IBUU results are listed in Table II in the column "N/Z IBUU prim." (IBUU primary fragment) and show fair agreement with the experimental results with the yield ratio fitting approach as well as the DIT simulation. In addition, the results are displayed in Fig. 6 and again show agreement with the experimental data. Additional work is needed to understand the differences that are seen between the IBUU results and the present data. Further efforts will aim at obtaining results with

the other parametrizations of the MDI mean-field potential and look for possible sensitivity of the calculations allowing one to obtain constraints on the isospin part of the effective interaction.

V. SUMMARY AND CONCLUSIONS

In summary, two approaches were used in this work to determine the average N/Z of quasiprojectiles and the ensuing degree of N/Z equilibration resulting from peripheral collisions of ^{40}Ca and ^{48}Ca projectiles at 32 MeV/nucleon interacting with ^{112}Sn and ^{124}Sn targets. The fragments produced from these collisions were efficiently collected with a charged-particle multidetector array allowing reconstruction of the corresponding quasiprojectiles. The first approach of quasiprojectile N/Z determination was based on the reconstruction using fully isotopically resolved fragments. This approach provided low N/Z values and was found to be seriously hindered by undetected neutrons. The second approach, developed in this work, is based on the assumption of early fragment formation and employs yield ratios of fragment isobars. This new approach was found to be unaffected by undetected neutrons. The determination of quasiprojectile N/Z allows the extraction of the degree of N/Z equilibration that occurred in the quasiprojectile (compared to a fully N/Z equilibrated system) and was found to be approximately 53%. The experimental results were compared with model calculations using two models. First, the phenomenological DIT model was used followed by SMM. The results of this calculation are in close agreement with the data and indicate that the mean number of undetected neutrons increases with the N/Z of the composite system and accounts for the difference observed between the two approaches of quasiprojectile N/Z determination. Second, the microscopic transport model IBUU was employed with a stiff parametrization of the density dependence of the symmetry energy, providing preliminary results in agreement with the data. It is concluded that the determination of the degree of N/Z equilibration employing the present fragment yield ratio approach may offer a sensitive probe to study the isospin part of the nuclear effective interaction when confronted with detailed calculations from microscopic models of the collisions in the Fermi energy regime.

ACKNOWLEDGMENTS

We thank A. Bonasera for insightful discussions and suggestions. We also thank the staff members of the Cyclotron Institute for the excellent beam quality and W. Meyer, L. Tassan-Got, and A. Botvina for the use of their codes. Funding was provided in part by the Department of Energy (Grant DE-FG03-93ER40773) and the Robert A. Welch Foundation (Grant A-1266). The Los Alamos Unlimited Release number is LA-UR-10-00054. M.V. acknowledges the support by the Slovak Scientific Grant Agency under Contract VEGA-2/0073/08.

[1] B. A. Li, L. W. Chen, and C. M. Ko, Phys. Rep. **464**, 113 (2008).
[2] D. V. Shetty, S. J. Yennello, and G. A. Souliotis, Phys. Rev. C **76**, 024606 (2007).
[3] J. R. Stone and P. G. Reinhard, Prog. Part. Nucl. Phys. **58**, 587 (2007).
[4] A. Steiner *et al.*, Phys. Rep. **411**, 325 (2005).
[5] L. W. Chen, C. M. Ko, and B. A. Li, Phys. Rev. Lett. **94**, 032701 (2005).
[6] M. B. Tsang *et al.*, Phys. Rev. Lett. **92**, 062701 (2004).
[7] M. B. Tsang and L. Shi, Nucl. Phys. A **738**, 115 (2004).
[8] V. Baran, M. Colonna, M. Di Toro, M. Zielinska-Pfabe, and H. H. Wolter, Phys. Rev. C **72**, 064620 (2005).
[9] B.-A. Li, C. B. Das, S. Das Gupta, and C. Gale, Phys. Rev. C **69**, 011603(R) (2004).
[10] B.-A. Li, C. B. Das, S. Das Gupta, and C. Gale, Nucl. Phys. A **735**, 563 (2004).
[11] Q. Li and Z. Li, Phys. Rev. C **64**, 064612 (2001).
[12] A. Hombach, W. Cassing, and U. Mosel, Eur. Phys. J. A **5**, 77 (1999).
[13] F. Rami *et al.*, Phys. Rev. Lett. **84**, 1120 (2000).
[14] E. Martin, R. Laforest, E. Ramakrishnan, D. J. Rowland, A. Ruangma, E. M. Winchester, and S. J. Yennello, Phys. Rev. C **62**, 027601 (2000).
[15] E. Bell, Ph.D. thesis, Texas A&M University, 2004.
[16] S. J. Yennello *et al.*, Phys. Lett. B **321**, 15 (1994).
[17] A. C. Merchant and W. Norenberg, Phys. Lett. B **104**, 15 (1981).
[18] H. Freiesleben and J. V. Kratz, Phys. Rep. **106**, 1 (1984).
[19] V. Baran, M. Colonna, V. Greco, and M. Di Toro, Phys. Rep. **410**, 335 (2005).
[20] G. A. Souliotis, M. Veselsky, D. V. Shetty, and S. J. Yennello, Phys. Lett. B **588**, 35 (2004).
[21] G. A. Souliotis *et al.*, Nucl. Phys. A **734**, 557 (2004).
[22] D. Rowland, Ph.D. thesis, Texas A&M University, 2000.
[23] D. Rowland *et al.*, Phys. Rev. C **67**, 064602 (2003).
[24] G. A. Souliotis *et al.*, Phys. Lett. B **543**, 163 (2002).
[25] G. A. Souliotis *et al.*, Phys. Rev. Lett. **91**, 022701 (2003).
[26] G. A. Souliotis *et al.*, Nucl. Instrum. Methods B **204**, 166 (2003).
[27] G. A. Souliotis *et al.*, Nucl. Instrum. Methods B **266**, 4692 (2008).
[28] H. Johnston *et al.*, Phys. Lett. B **371**, 186 (1996).
[29] A. L. Keksis, Ph.D. thesis, Texas A&M University, 2007.
[30] F. Gimeno-Nogues *et al.*, Nucl. Instrum. Methods A **399**, 94 (1997).
[31] L. Tassan-Got, Nucl. Instrum. Methods B **194**, 503 (2002).
[32] W. G. Meyer, DONNA Program, University of Maryland, 1978 (unpublished program).
[33] A. Barranon *et al.*, Rev. Mex. De Fis. **45**, 110 (1999).
[34] N. Marie *et al.*, Phys. Rev. C **58**, 256 (1998).
[35] D. V. Shetty *et al.*, Phys. Rev. C **68**, 054605 (2003).
[36] M. Veselsky *et al.*, Phys. Lett. B **497**, 1 (2001).
[37] M. B. Tsang *et al.*, Phys. Rev. C **64**, 054615 (2001).
[38] A. S. Botvina, O. V. Lozhkin, and W. Trautmann, Phys. Rev. C **65**, 044610 (2002).
[39] L. Tassan-Got and C. Stephan, Nucl. Phys. A **524**, 121 (1991).
[40] M. Veselsky *et al.*, Phys. Rev. C **62**, 064613 (2000).
[41] M. Veselsky *et al.*, Nucl. Phys. A **724**, 431 (2003).
[42] J. P. Bondorf, A. S. Botvina, A. S. Iljinov, I. N. Mishustin, and K. Sneppen, Phys. Rep. **257**, 133 (1995).

[43] A. S. Botvina *et al.*, Nucl. Phys. A **475**, 663 (1987).
[44] A. S. Botvina, A. S. Iljinov, and I. N. Mishustin, Nucl. Phys. A **507**, 649 (1990).
[45] A. S. Botvina, A. D. Jackson, and I. N. Mishustin, Phys. Rev. E **62**, R64 (2000).
[46] A. S. Botvina and I. N. Mishustin, Phys. Rev. C **63**, 061601(R) (2001).
[47] G. A. Souliotis, A. S. Botvina, D. V. Shetty, A. L. Keksis, M. Jandel, M. Veselsky, and S. J. Yennello, Phys. Rev. C **75**, 011601(R) (2007).
[48] M. Veselsky and G. A. Souliotis, Nucl. Phys. A **765**, 252 (2006).
[49] C. Hartnack *et al.*, Eur. Phys. J. A **1**, 151 (1998).
[50] A. Ono and J. Randrup, Eur. Phys. J. A **30**, 109 (2006).